

Experimental Measurements of the Compressibility, Temperature, and Light Absorption in Dense Shock-Compressed Gaseous Deuterium

S. K. Grishechkin¹, S. K. Gruzdev¹, V. K. Gryaznov^{2, **}, M. V. Zhernokletov^{1, *},
R. I. Il'kaev¹, I. L. Iosilevskii³, G. N. Kashintseva¹, S. I. Kirshanov¹, S. F. Manachkin¹,
V. B. Mintsev², A. L. Mikhailov¹, A. B. Mezhevov¹, M. A. Mochalov¹, V. E. Fortov²,
V. V. Khrustalev¹, A. N. Shuikin¹, and A. A. Yukhimchuk¹

¹ Russian Federal Nuclear Center, All-Russia Research Institute of Experimental Physics, Sarov,
Nizhni Novgorod region, 607190 Russia

*e-mail: root@gdd.vniief.ru

² Institute of Problems of Chemical Physics, Chernogolovka Branch, Russian Academy of Sciences,
Chernogolovka, Moscow region, 142432 Russia

**e-mail: grvk@icp.ac.ru

³ Moscow Institute of Physics and Technology, Institutskii per. 9, Dolgoprudnyi, Moscow region, 141700 Russia

Received August 5, 2004

Experimental data on the shock compression, temperature, and absorptivity of gaseous deuterium with an initial density close to its value in the liquid state were obtained on a spherical explosion shock-wave generator in a pressure range of 80–90 GPa. The obtained results are compared with the existing experimental and theoretical data. © 2004 MAIK “Nauka/Interperiodica”.

PACS numbers: 52.25.-b; 52.35.Tc

At present, advances in laser fusion and progress in the understanding of the structure and evolution of astrophysical objects have quickened interest in the study of thermodynamic and electrophysical properties of hydrogen—the simplest and most abundant element in nature—in the megabar pressure range [1, 2]. To achieve shock-compression megabar pressures, various methods of shock-wave excitation are used: intense laser radiation [3, 4], high-power pulse currents [5, 6], and spherical explosion devices [2, 7]. Although the laser data demonstrate anomalously high compressibility of deuterium plasma, this was not confirmed by the electrodynamic and explosion experiments.

In this work, gaseous deuterium with a high initial density, close to the density of liquid deuterium, was chosen as the object of investigation. The use of gaseous deuterium was dictated by the possibility of obtaining its initial parameters with a high certainty, because they are fully determined by the initial gas pressure and temperature. Besides, the temperature and light absorption coefficients were measured in this work simultaneously with the compressibility, allowing additional information to be gained on the parameters of the state and optical properties of the shock-compressed deuterium plasma.

Experimental measurements of dynamic characteristics. For the experiments with gaseous deuterium under a high initial pressure, a hemispherical capsule

was devised (Fig. 1), whose geometrical sizes corresponded to a hemispherical shock-wave generator MZ-13 [8]. Capsule frame 1 and base 2 were made from a high-strength steel possessing high stability of its characteristics in a hydrogen atmosphere. To

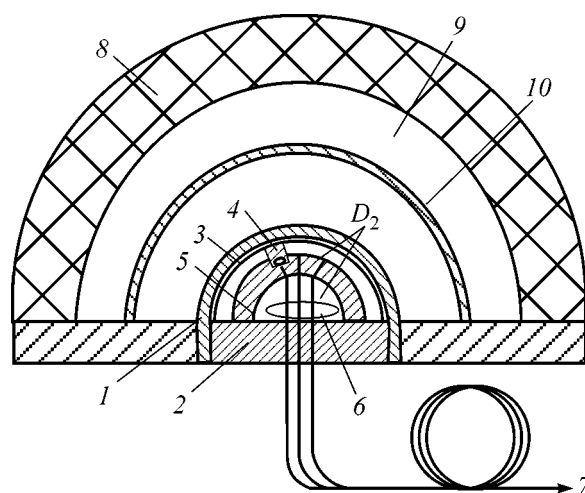


Fig. 1. Hemispherical experimental device: (1) frame; (2) base; (3) screen (aluminum AD-1); (4) aluminum (AD-1) sample; (5) housing; (6) optical sensors; (7) measuring line; (8) explosive; (9) air gap; (10) impactor (steel 3).

enhance the shock-compression pressure in deuterium, hemispherical 1.5-mm-thick aluminum (AD-1) screen 3 was placed under steel frame 1.

At a fixed distance (determined by the height of aluminum samples 4) from the aluminum screen, hemispherical brass housing 5 was mounted, inside which eight optical sensors 6 for measuring shock velocity in deuterium were symmetrically arranged on a circle with radius $R = 5$ mm. Similar sensors were also placed beneath the samples to measure shock velocity in them and use this velocity for determining the shock-compression parameters in the aluminum screen. The sensors were fabricated from 200- μm o.d. silica fibers with several-micron-thick aluminum jackets along the whole length to eliminate spurious illumination. The fibers were glued in base 2 and brass hemisphere 5; their polished top ends were mounted flush with the outer surface of the hemisphere. The bottom (in the scheme) ends terminated in the optical connector (not shown in the figure) for joining the optical sensors to external fiber lines 7, through which the shock-front radiation was transmitted to detectors. The central fiber, with a diameter of 600 μm , served also for measuring the shock velocity in gas and the shock-front temperature.

After the initiation of potent explosive 8, steel hemispherical impactor 10 was accelerated through gap 9 by the explosion products to form, upon the collision with hemispherical frame 1, a shock wave in it, that was then sequentially transmitted to the aluminum housing of sensors 6 and to the gaseous deuterium. The latter was compressed and irreversibly heated. To eliminate the influence of the shock wave on the experimental results, air from the space between frame 1 and impactor 10 was pumped out to a residual pressure of no higher than 10 torr.

The capsule was filled with gaseous deuterium from a metal-hydride source of high-pressure vanadium-based hydrogen isotopes. To achieve a pressure of 250 MPa using the vanadium-deuteride source, it suffices to heat it to a temperature of ~ 450 K [9].

Before the experiments, the capsules were tested for strength and tightness. The tests showed that the capsules withstood up to a gas pressure of ~ 220 MPa without destruction and noticeable residual deformations of the construction. During the course of testing, deformation of hemisphere floors was detected, and it was subsequently taken into account in the processing of the experimental results.

Two experiments, with the initial gas parameters $P_0 \approx 203$ MPa (2000 atm) and $T_0 = 273$ K in the first experiment and $P_0 \approx 157$ MPa (1550 atm) and $T_0 = 278$ K in the second, were performed using shock-wave generators of the same type. The gas temperature was assumed to be equal to the temperature measured by a thermocouple at the hemispherical capsule surface. Under these conditions, the initial gas densities calculated according to [10] were $\rho_0 = 0.153$ g/cm³ and $\rho_0 =$

0.1335 g/cm³, respectively, which is close to the density of liquid deuterium ($\rho_0 = 0.171$ g/cm³).

The shock-front glow was detected in the visible region by optical transducers based on photodiodes with a signal rise time no worse than 2 ns and photomultipliers with an anode-pulse rise time of 1.2 ns. The shock-wave passage time was measured from the instant of glow appearance to the instant of glow decay due to the damage of the fiber end by the shock wave. The typical oscillograms of the shock-front glow in gaseous deuterium are shown in Fig. 2. The brightness temperature of shock-compressed deuterium was determined from the glow amplitude (Fig. 2b) in the saturation region.

The measurements of the average shock velocities in dense gaseous deuterium gave $D_{\text{exp}} = (29.14 \pm 0.56)$ km/s at $P_0 > 203$ MPa (2000 atm) and $D_{\text{exp}} = (29.29 \pm 0.36)$ km/s at $P_0 \approx 157$ MPa (1550 atm). The measurement error was determined using Student statistics with a fiducial probability of 90%. The experimental values of the average shock velocity corresponded to the middle of the gauge length, and, to reduce them to the shock-decay boundary at the deuterium–aluminum interface (Fig. 1), corrections were introduced. To this end, one-dimensional calculations of the shock motion in the elements of the experimental hemispherical device were performed using the gas-dynamic program developed at the Russian Federal Nuclear Center, All-Russia Research Institute of Experimental Physics. For the deuterium calculations, the equation of state was borrowed from [11], and the equations of state for the remaining materials were those used at the Institute. To assess the correctness of the equations of state used in the program for the materials of the device, an independent test of the computational scheme was carried out. In the test calculations, the shock velocities in 4-mm-thick iron and aluminum screens were estimated and the results were compared with the experimental data for MZ-13 in [8]. The testing showed that shock velocities calculated for iron and aluminum agree, to within 1%, with the experimental data $D_{\text{Fe}} = 17.35$ km/s and $D_{\text{Al}} = 20.9$ km/s [8].

The transition from the measured shock velocities to their instant values corresponding to the shock-decay boundary at the aluminum–deuterium interface was done as follows. The results of gas-dynamic computations were used to calculate the average shock velocities \bar{D} in deuterium and the velocities D_b at the screen–deuterium boundary. Since the shock wave in a hemispherical generator is nonstationary, the average velocity on the measurement radius exceeds the velocity D_b at the inner boundary of the screen. With allowance made for the relative difference between the values $\delta D = (\bar{D} - D_b)/\bar{D}$ obtained from the computational results, the corrections $\Delta D = \delta D D_{\text{exp}}$ to the experimentally measured shock velocity were calculated. The resulting shock velocities in gaseous deuterium became

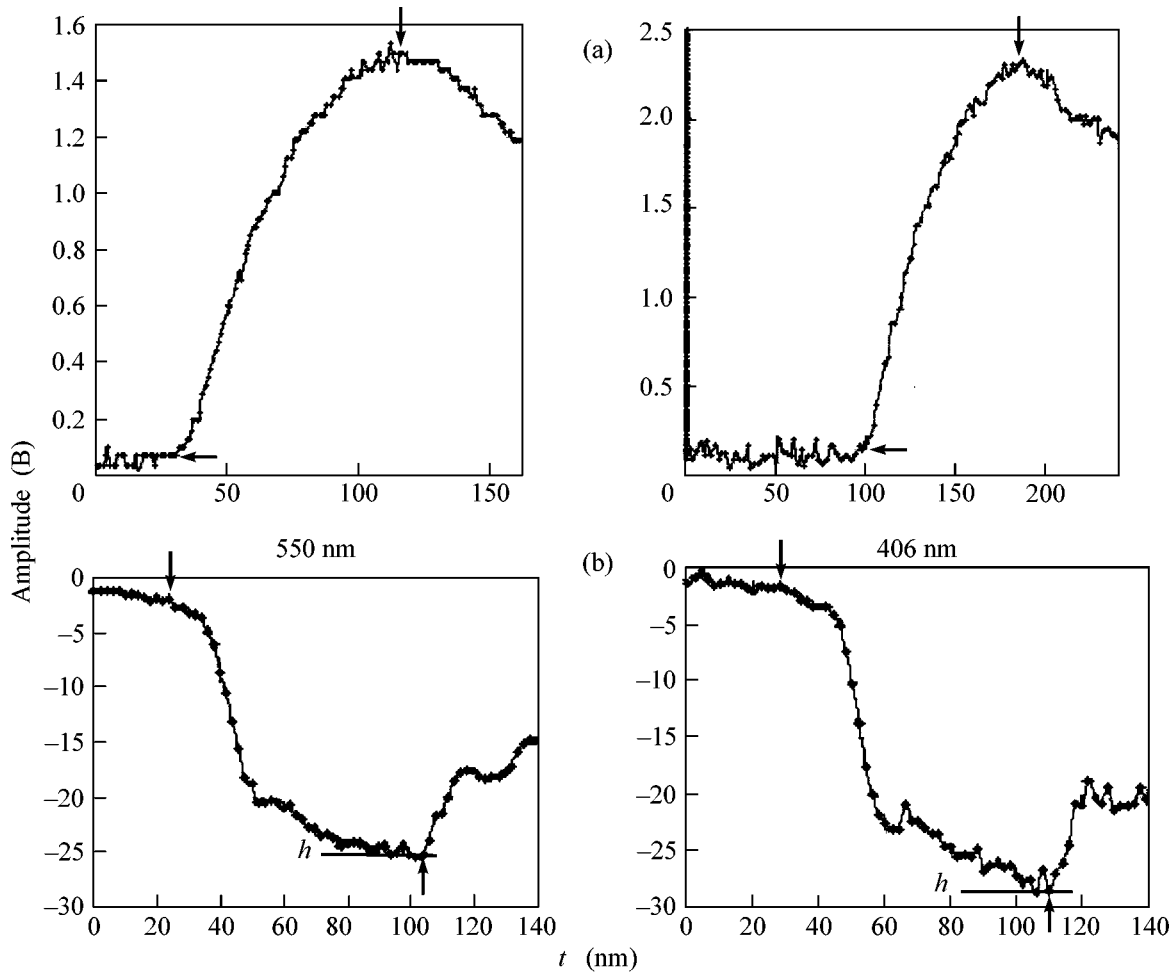


Fig. 2. Shock-front radiation oscillograms for gaseous deuterium. Detectors: (a) photodiode sensors and (b) photomultipliers. Arrows show the points at which the time of shock-wave motion was measured.

reduced to its boundary with aluminum: $D_b = 27.95$ km/s in the first experiment and $D_b = 28.02$ km/s in the second.

The correction to the average shock velocity $D_{\text{exp}} = 21.17$ km/s measured in the experiments with reference aluminum samples was done in a similar way. The corrected shock velocity in aluminum at the boundary with deuterium was found to be $D_b(\text{Al}) = 20.4$ km/s.

The solution to the problem of shock decay at the deuterium–aluminum boundary with the indicated velocities and the use of the law of conservation of mass bring about the following shock-compression parameters for gaseous deuterium: $D = 27.95$ km/s (shock velocity), $U = 21.84$ km/s (mass velocity), $P = 93.4$ GPa, and $\rho = (0.70 \pm 0.06)$ g/cm³ in the first experiment and $D = 28.02$ km/s, $U = 22.2$ km/s, $P = 83$ GPa, and $\rho = (0.64 \pm 0.04)$ g/cm³ in the second. To solve the problem, an aluminum unloading isentrope was constructed using the equation of state given in [12]. The initial state on the Hugoniot curve had parameters $U = 12.04$ km/s and $P = 665.4$ GPa that were obtained from

the shock-velocity measurements in aluminum ($D_b(\text{Al}) = 20.4$ km/s).

Measurements of the optical characteristics of shock-compressed deuterium. The temperature of shock-compressed deuterium was measured using a high-speed four-channel optical pyrometer [13]. The radiation of the shock front in deuterium was recorded via the fiber line at wavelengths of 450, 498, 550, and 600 nm. To separate the corresponding spectral intervals, a set of interference light filters with a transmission bandwidth at half maximum $\Delta\lambda \approx 10$ nm was used. Prior to the experiments, the optical line for measuring temperature was calibrated against a reference light source. The thermal radiation flux from a heated body with the radiating capacity R is given by the Planck's formula,

$$N(\lambda) = RC_1\lambda^{-5}[\exp(C_2/\lambda T) - 1]^{-1} \\ = C_1\lambda^{-5}[\exp(C_2/\lambda T_b) - 1]^{-1}. \quad (1)$$

Table

Experiment				Calculations (chemical model [1, 23])							Experiment
ρ_0 , g/cm ³	P , GPa	ρ , g/cm ³	T , 10 ³ K	T , 10 ³ K	n_e , 10 ²² /cm	n_D , 10 ²² /cm	n_{D2} , 10 ²² /cm	Γ_D	$n_e \lambda_e^3$	$\pi(\sum n_j g_j^3)/6$	
0.134	83	0.64	22.9	23.2	2.3	5.1	5.6	15	2.7	0.42	This work
0.153	93.4	0.70	24.1	22.5	2.5	5.0	6.6	16	3.0	0.47	This work
0.171	107	0.77	–	23.0	2.8	5.3	7.1	17	3.4	0.50	[25]
0.199	121	0.85	–	21.9	3.0	4.9	8.5	18	3.8	0.57	[7]

Here, R is the radiating capacity of the body, λ is the wavelength, T is the actual temperature, T_b is the brightness temperature, and the constants are $C_1 = 1.19 \times 10^{-16}$ (W m²)/sr and $C_2 = 0.0144$ mK. The temperature of the shock-compressed gaseous deuterium was determined from the four measured spectral temperatures by the nonlinear least-squares method for two parameters T and R , followed by iterations to obtain exact estimates for the quantities of interest.

At the spectral temperatures experimentally measured for the shock-compression pressure $P = 93.4$ GPa in the range 450–600 nm, the best fit to the Planck's function is achieved, in the grey-body approximation, at the temperature $T = 24\,100 \pm 2200$ K and a radiating capacity of 0.485 ± 0.075 .

Analysis of the oscillograms obtained in the experiment with pressure $P = 83$ GPa (Fig. 2b) indicates that the saturation of the shock-front radiation corresponding to the optical thickness (close to unity) of shock-compressed gaseous deuterium is not achieved in the blue spectral region ($\lambda = 406$ nm). Since this does not allow the use of the least-squares method for estimating the actual temperature and radiating capacity, only the average value $T = 22\,900 \pm 2000$ K of the brightness temperature was presented for this experiment.

As in [14, 15], the rise of the shock-front glow after the wave enters gaseous deuterium can be due to the increase in the thickness of the shock-compressed layer and to its transparency. Neglecting the reflection and using the Bouguer–Lambert–Beer formula for transmittance,

$$\tau = \exp(-\alpha l), \quad (2)$$

where α is the absorption coefficient of a layer of thickness l , one can write the rise of radiation intensity in the normal direction as

$$\begin{aligned} I &= I_0[1 - \exp(-\alpha l)] \\ &= I_0[1 - \exp(-\alpha\{D - U\}t)], \end{aligned} \quad (3)$$

where I_0 is the radiation intensity of an optically dense layer, $l = (D - U)t$ is the thickness of a shock-compressed substance, and t is the shock-wave passage time in the substance. Then, with the known kinematic parameters D and U , one can use the experimental

oscillogram to determine the light absorption coefficient α in the shock-compressed deuterium:

$$\alpha = -I_0[1/(D - U)t] \ln(1 - I/I_0). \quad (4)$$

The average value of this coefficient obtained for the compressed gaseous deuterium after processing the experimental oscillograms was found to be $\alpha \approx 69$ cm⁻¹ in the wavelength range 450–600 nm for a shock compression of 93 GPa.

The estimates made for the absorption coefficient within the framework of the classical approach using the calculated parameters and the Kramers–Unsold formula give $\alpha \approx 4 \times 10^4$ cm⁻¹, which is three orders of magnitude larger than the measured values. Such a discrepancy is evidence that the ionization and dissociation processes at the shock front likely bypass the rise of the plasma-bunch radiation.

Comparison with the results of theoretical calculations. Our experiments differ from the majority of previous experiments in that the dynamic compression characteristics fixing the position of the Hugoniot curve in the P – V plane are measured simultaneously with the temperature of the shock-compressed deuterium, which is highly important for the construction of a complete thermodynamic map for the system.

The experimental results are presented in the table and Fig. 3 in the pressure–density coordinates and, in the temperature–pressure coordinates, in the same table and Fig. 4, together with the available experimental data and the results of theoretical calculations in two variants.

In the first variant, the calculations were carried out using the equation of state constructed for hydrogen within the relatively simple compressible covolume model (CCM) [11]. A mixture of five sorts of particles was considered: molecules, atoms, positive molecular ions, protons, and electrons. The thermal equation of state for the particle of the i th sort has the form $V_i(P, T) = V_{C,i}(P) = R_m T/P$, where V is the molar volume and R_m is the molar gas constant. The covolumes $V_{C,i}$ were assumed to depend only on pressure and be additive. For molecules, the covolume was constructed using the experimental data on the static compression of solid hydrogen up to a pressure of 2.5 GPa [16] and quasi-adiabatic compression of gaseous hydrogen in

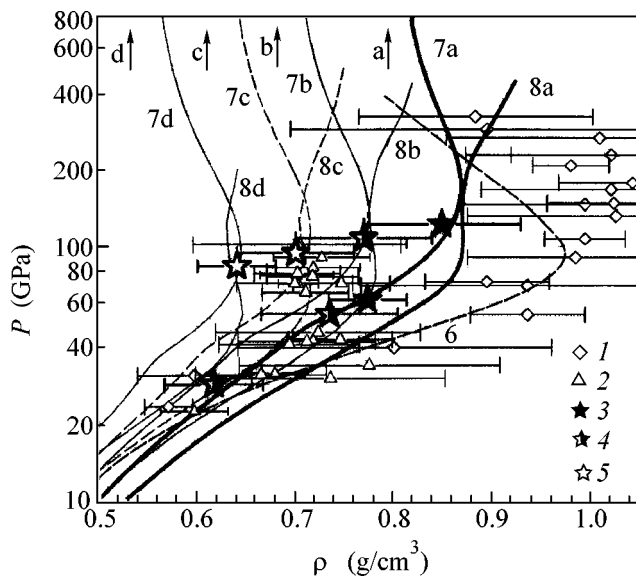


Fig. 3. Deuterium Hugoniot adiabats. Experiment: (1) [3], (2) [6], (3) [2, 7], (4) [25], and (5) this work. Calculations: (6) [27], (7) SAHA-IV [1, 23], (8) CCM [11], solid thick line for $\rho_0 = 0.199$ g/cm³, solid thin line for $\rho_0 = 0.171$ g/cm³, dash-and-dot line for $\rho_0 = 0.153$ g/cm³, and the dotted line for $\rho_0 = 0.1335$ g/cm³. Arrows indicate the "limiting" compressions ($\rho/\rho_0 = 4$) for each of the four Hugoniot curves.

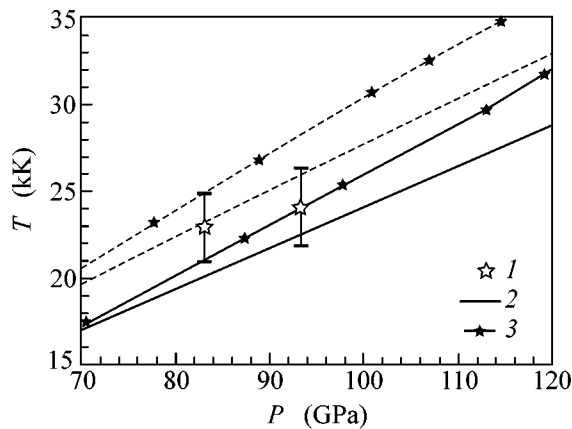


Fig. 4. Pressure dependence of the temperature of shock-compressed gaseous deuterium: (1) experiment; calculation: (2) SAHA-IV model [1, 23], (3) CCM model [11]; solid lines are for $\rho_0 = 0.153$ g/cm³ and dashes are for $\rho_0 = 0.1335$ g/cm³.

the pressure range 40–800 GPa [17, 18]. For atoms, the covolume was constructed using simple theoretical estimates and experimental results for $P > 300$ GPa [17, 18]. For molecular ions and protons, they were taken to be formally equal to the covolumes of, respectively, molecules and atoms (for electrons, $V_{C,e}(P) \equiv 0$). The caloric equation of state was obtained from the thermal

equation using the second law of thermodynamics. The contribution from the vibrational and rotational degrees of freedom of molecules and molecular ions in the partition functions was taken into account in the "rigid rotator–harmonic oscillator" approximation, without rovibrational cutoff at the level of dissociation energy, while the contribution from the excited electronic states was disregarded. The equations for the equilibrium concentrations of the components have the form of the usual Saha equations, in which the equilibrium constant is additionally multiplied by the factor $\exp(-\Delta G_{C,r}(P)/RT)$, where $\Delta G_{C,r}$ is a change in the covolume chemical potential in the r th reaction. As a result, the energy of molecular dissociation into two atoms formally decreases by $\Delta G_{C,dis}(P) = 2G_{C,D}(P) - G_{C,D_2}(P)$ with the pressure buildup, whereas the ionization potentials of molecules and atoms do not change by virtue of the definition adopted above for the covolumes of charged particles. For the states achieved in our experiments, the CCM calculations predict a noticeable degree, $n_D/n_{D_2} \sim 3$, of deuterium dissociation and a relatively low degree, $n_{D^+}/n_D \sim 10^{-2}$, of temperature ionization. The CCM-calculated Hugoniot curves show two density maxima: the lower corresponds to the molecular dissociation, and the upper corresponds to the particle ionization. The position of the second maximum can be affected by many factors. In particular, the rovibrational cutoff at the level of dissociation energy of molecular ions leads to a decrease in the concentration of this component in the mixture at high temperatures and pressures and, as a result, to a noticeable decrease in the density and pressure at the upper maximum and to a steeper asymptotic form of the Hugoniot adiabat $\rho_{Hug} \rightarrow 4\rho_0$.

In the second variant, the calculations were performed using a modified plasma chemical model [19] with the universal SAHA-IV code [20]. In this model, hydrogen (deuterium) was calculated as a strongly non-ideal mixture of ions, electrons, atoms, molecules, and D^- and D^{2+} ions. When calculating the equilibrium plasma composition and its thermodynamic properties, the partial degeneracy of the electronic component and the interactions between all sorts of particles were taken into account. To describe the coulombic nonideality, an improved modification of the pseudopotential approach suggested in [21] was used. With this modification, the effective electron–ion interaction was described by the short-range-corrected Coulomb potential (Glauber–Yukhnovskii potential). The effective depth of this potential was taken as equal to the interaction energy of an electron–ion pair at the average distance between heavy particles (ions, atoms, and molecules). This corresponds to the cutoff energy adopted in this model for separating the free and bound (intra-atomic) states in the calculation of atomic partition functions. Apart from the contribution from the Coulomb interaction between charged particles, the strong repulsion of heavy particles at close distances [20] was

taken into account. This was accomplished using the approximate equation of state for “soft spheres” [22], modified to a mixture of particles with different diameters. The degree of softness of the intermolecular repulsion potential was chosen from the requirement of the best description of the experimentally measured equation of state for condensed hydrogen at room temperature. The calculations in this approximation [1, 23] showed not only the dominant role of the D_2 – D_2 interaction but also that the position of the deuterium Hugoniot adiabat and the temperature dependences on the adiabat are highly sensitive to the choice of the D – D and, notably, D – D_2 repulsion parameters. In our calculations (part of them are summarized in the table), the parameters of the intermolecular and interatomic repulsions were chosen according to the *ab initio* atom–atom approximation [24]. In terms of the model of soft spheres, this leads to a relatively high ratio of the effective diameter of deuterium atom to the diameter $D_2\{d(D)/d(D_2) \sim 0.8\}$. An important consequence of this choice is that the “self” volumes of the reaction products show no appreciable change during the deuterium dissociation process and, correspondingly, there is no mechanism that would stimulate the pressure-induced dissociation in a strongly compressed equilibrium system of molecules and atoms at the expense of the gain in self-volume.

Calculations in the modified plasma chemical model [1, 19, 23] show that the states arising behind the shock-wave front in this work and in the experiments with maximal pressure [2, 7] correspond to a dense strongly nonideal ($\Gamma_D \approx 1$), partially ionized ($n_e/n_D \sim 1$), partially degenerate ($n_e\lambda_e^3 \sim 3$), and practically isothermic ($T \approx 22$ – 24 kK) deuterium plasma with parameters given in the table.

An analysis of the data presented in the table shows that the physical conditions realized in the shock experiments at the Institute of Experimental Physics are distinguished by a combination of strong coulombic nonideality ($\Gamma_d \gg 1$), electron-component degeneracy ($n_e\lambda_e^3 \sim 1$), and strong influence of the short-range repulsion that manifests itself in the high values of the so-called packing parameter $\pi n_i d_i^3/6 \sim 1$ (d_i is the self-size of a heavy particle of the i th sort (atom, molecule, etc.)).

One can see in Fig. 3 that the experimental data obtained in this work agree well with the data calculated on the basis of the CCM and SAHA-IV models. It is worthy of note that these theoretical models agree simultaneously both with the results of our experiments on the shock compression of a preliminarily compressed gaseous deuterium and with the results of the shock compression of liquid and solid deuterium [2, 7, 25]. This suggests that the results of all shock-wave experiments conducted at the Institute of Experimental Physics are mutually consistent. Nevertheless, the fact that, although the Hugoniot adiabates in both theoretic-

cal models tend to the ideal-gas asymptotic compression limit $\rho_{\text{Hug}}/\rho_0 \rightarrow 4$ [26] at the high-pressure and high-temperature limits, the character of this tendency is different for both models. This renders the necessity of obtaining new experimental data in the pressure range ~ 0.2 – 1.0 TPa topical and necessitates the use of *ab initio* calculations for determining the thermodynamic functions of dense hydrogen (deuterium) plasma.

From the comparison (Fig. 4) of the experimentally determined and calculated temperatures, it follows that, as earlier, the experimental results obtained in this agree satisfactorily with the results of both CCM and SAHA-IV calculations. It should be noted that the coincidence of the theory and experiment for the caloric and thermal equations of states indicates, first, that the theoretical models are adequate and, on the other hand, that the experimental data obtained in this work are self-consistent.

This work was supported in part by the complex program “Thermal Physics and Mechanics of Intense Pulsed Actions,” a Presidential Grant (no. (NSh-1938.2003.2), and a State Contract of the Ministry of Education and Science of the Russian Federation (no. 40.009.1.1.1192).

REFERENCES

1. V. E. Fortov, V. Ya. Ternovoi, M. V. Zhernokletov, *et al.*, Zh. Éksp. Teor. Fiz. **124**, 288 (2003) [JETP **97**, 259 (2003)].
2. S. I. Belov, G. V. Boriskov, A. I. Bykov, *et al.*, Pis'ma Zh. Éksp. Teor. Fiz. **76**, 508 (2002) [JETP Lett. **76**, 433 (2002)].
3. L. D. Da Silva, P. Gelliers, G. W. Collins, *et al.*, Phys. Rev. Lett. **78**, 483 (1997).
4. A. N. Mostovych, Y. Chan, T. Lehecha, *et al.*, Phys. Rev. Lett. **85**, 3870 (2000).
5. D. L. Hanson, J. R. Asay, C. A. Hall, *et al.*, in *Shock Compression of Condensed Matter*, Ed. by M. D. Furnish, L. C. Chhabildas, and R. S. Hixson (Am. Inst. of Physics, Melville, N.Y., 1999), p. 1175.
6. M. D. Knudson, D. L. Hanson, J. E. Bailey, *et al.*, Phys. Rev. Lett. **87**, 225501 (2001); Phys. Rev. Lett. **90**, 035505 (2003); Phys. Rev. B **69**, 144 209 (2004).
7. G. V. Boriskov, A. I. Bykov, R. I. Il'kaev, *et al.*, Dokl. Akad. Nauk **392**, 755 (2003) [Dokl. Phys. **48**, 553 (2003)].
8. L. V. Al'tshuler, R. F. Trunin, K. K. Krupnikov, and N. V. Panov, Usp. Fiz. Nauk **166**, 575 (1996) [Phys. Usp. **39**, 539 (1996)].
9. A. N. Golubkov and A. A. Yukhimchuk, Hyperfine Interact. **138**, 403 (2001).
10. A. Michels, W. de Graff, T. Wassenaar, *et al.*, Physica (Amsterdam) **25**, 25 (1959).
11. V. P. Kopyshv and V. V. Khrustalev, Prikl. Mekh. Tekh. Fiz., No. 1, 122 (1980).

12. B. L. Glushak, L. F. Gudarenko, Yu. M. Styazhkin, and V. A. Zherebtsov, *Vopr. At. Nauki Tekh., Ser.: Mat. Model. Fiz. Protssessov*, No. 1, 32 (1991).
13. M. A. Mochalov, T. S. Lebedeva, A. B. Medvedev, *et al.*, in *Proceedings of 12th APS Topical Group Meeting on Shock Compression of Condensed Matter*, Ed. by Donna M. Baudrau (CMP, Atlanta, Georgia, 2001); *Bull. Am. Phys. Soc.* **46** (4), 60 (2001).
14. S. B. Kormer, *Usp. Fiz. Nauk* **94**, 641 (1968) [*Sov. Phys. Usp.* **11**, 229 (1968)].
15. V. D. Glukhodedov, S. I. Kirshanov, T. S. Lebedeva, and M. A. Mochalov, *Zh. Éksp. Teor. Fiz.* **116**, 551 (1999) [*JETP* **89**, 292 (1999)].
16. M. S. Anderson and C. A. Swenson, *Phys. Rev. B* **10**, 5184 (1974).
17. F. V. Grigor'ev, S. B. Kormer, O. L. Mikhaïlova, *et al.*, *Pis'ma Zh. Éksp. Teor. Fiz.* **16**, 286 (1972) [*JETP Lett.* **16**, 201 (1972)].
18. F. V. Grigor'ev, S. B. Kormer, O. L. Mikhaïlova, *et al.*, *Zh. Éksp. Teor. Fiz.* **69**, 743 (1975) [*Sov. Phys. JETP* **42**, 378 (1975)].
19. *Thermal Properties of Working Media of Gas-Phase Nuclear Reactor*, Ed. by V. M. Ievlev (Atomizdat, Moscow, 1980) [in Russian].
20. V. K. Gryaznov, I. L. Iosilevskii, and V. E. Fortov, in *Shock Waves and Extreme States of Matter*, Ed. by V. E. Fortov, L. V. Al'tshuler, R. F. Trunin, and A. I. Funtikov (Nauka, Moscow, 2000; Springer, New York, 2004).
21. I. L. Iosilevskii, *Teplofiz. Vys. Temp.* **18**, 355 (1980).
22. D. Young, *Soft Spheres Model for Equation of State*, LLNL Report (Univ. of California, 1977), UCRL-52352.
23. V. K. Gryaznov, I. L. Iosilevskii, and V. E. Fortov, in *Physics of Extreme States of Substance-2001*, Ed. by V. E. Fortov (IKhPF, Chernogolovka, 2001), p. 114 [in Russian].
24. E. S. Yakub, *Teplofiz. Vys. Temp.* **28**, 664 (1990); *Physica B (Amsterdam)* **265**, 31 (1999).
25. G. V. Boriskov, A. I. Bykov, R. I. Il'kaev, *et al.*, *Phys. Rev. B* (in press).
26. Ya. B. Zel'dovich and Yu. P. Raizer, *Physics of Shock Waves and High-Temperature Hydrodynamic Phenomena*, 2nd ed. (Nauka, Moscow, 1966; Academic, New York, 1967).
27. M. Ross, *Phys. Rev. B* **58**, 669 (1998).

Translated by V. Sakun